# GLACIAL HYDROCLIMATE OF WESTERN NORTH AMERICA: INSIGHTS FROM PROXY-MODEL COMPARISON AND IMPLICATIONS FOR LAKE BONNEVILLE

Jessica L. Oster[1] and Daniel E. Ibarra[2]

[1]Department of Earth and Environmental Sciences, Vanderbilt University, 5726 Stevenson Center, 7th Floor, Nashville, TN 37240;
[2]Department of Geological Sciences, Stanford University, 450 Serra Mall, Building 320, Stanford, CA 94305-2115

Corresponding author (Oster): jessica.l.oster@vanderbilt.edu

## ABSTRACT

Decades of paleoclimate research have helped bring the pattern of hydroclimatic change across North America during the Last Glacial Maximum (LGM) into ever sharper focus. Despite these advances, the drivers of LGM hydroclimatic variability continue to be debated at the continental to basin scale. To explore the driving mechanisms behind LGM hydroclimatic change, we compare an updated network of moisture sensitive LGM proxy records from across North America and northern Central America with the annual precipitation output of nine simulations of LGM climate conducted as part of the Paleoclimate Model Intercomparison Project, as well as an ensemble average. The updated proxy network presented here points to wetter than modern conditions across most of the southwestern United States, with drier than modern conditions in the Pacific Northwest, Rocky Mountains, and parts of the Colorado Plateau. We find that, similar to previous work, the degree of model agreement with the proxy network is sensitive to the location and orientation of the simulated boundary between wetter and drier conditions in the western United States. The Bonneville basin occupies a key position in this context, as it is within this transition between wetter and drier conditions during the LGM. Proxy records from within and around the Bonneville basin suggest conditions that were unchanged or slightly wetter during the LGM, and the models that show the best agreement with the proxy network overall place the transition between wet and dry LGM precipitation anomalies at or near Lake Bonneville. Although models do not include pluvial lakes in their boundary conditions, our computed effective moisture anomalies as well as the model set up variables for IPSL-CM5A-LR and NCAR CCSM4, two of the models that best agree with the proxy network, demonstrate that at least these two models do include the present-day Great Salt Lake. These two models show weak positive precipitation anomalies downwind of the modern lake area and in general show good agreement with Bonneville basin proxy records. This suggests that future inclusion of pluvial lakes in model boundary conditions for the LGM could both improve proxy-model agreement and enhance our understanding of how processes such as vapor recycling influence the hydroclimate of continental interiors.

## INTRODUCTION AND METHODOLOGY

Western North America has experienced a dynamic hydroclimatic history over the last glacial cycle, recorded by the growth and desiccation of large inland lakes, expansions and contractions in the ranges of vegetation, and variations in the chemical composition of pedogenic and cave minerals (Nowak and others, 1994; Maher and others, 2014; Reheis and others, 2014). More than a century of paleoclimatic research in this region has provided a wealth of information about the spatial and temporal patterns of these changes, and important insight into the drivers of hydroclimatic change can be gained by integrating these records and comparing them with paleoclimate model simulations. A network of moisture-sensitive proxies as well as pollen-based precipitation and moisture reconstructions suggest a dipole pattern across this region at the Last Glacial Maximum (LGM, ~21 ka), with a wet southwest and dry conditions approaching the Laurentide Ice Sheet (Oster and others, 2015). Yet despite a relatively clear picture of glacial climate in western North America, the atmospheric drivers behind these patterns remain a source of debate (Lyle and others, 2012; Lora and others, 2017; Morrill and others, 2018). Early modeling studies suggested that the westerly storm track was shifted southward during LGM (COHMAP Members, 1988) while more recent work has indicated that rather than a uniform southward shift, the storm track was steered in a northwest-southeast direction across the region by high pressure situated over the Laurentide Ice Sheet (Oster and others, 2015). Other work has pointed to the importance of an influx of sub-tropically derived southwesterly winter moisture in setting up this regional pattern (Lora and others, 2017). Our understanding of glacial hydroclimate is further complicated by the pattern of hydroclimatic change across western North America following the LGM, as the majority of western pluvial lakes achieve higher levels during Heinrich Stadial 1 (18–15

ka) or later as the Laurentide Ice Sheet is decaying (for example, Munroe and Laabs, 2013; Ibarra and others, 2014).

Here, we draw upon the large body of proxy evidence and recent modeling work to provide the most up to date snapshot of glacial hydroclimatic change in the Bonneville basin and western North America broadly. We have compiled an updated network of moisture sensitive proxy records from western North America, and expanded this network to include all of North America. The present compilation builds upon our previous work (Oster and others, 2015) through the addition of recently published records that include pollen and macrofossil-based estimates of hydroclimatic change (Scheff and others, 2017; Harbert and Nixon, 2018) as well as new records and modeling local to the Bonneville basin (Quirk and others, 2018; Ibarra and others, 2019). We have expanded our proxy network, previously compiled for western North America, to include all of North America as well as northern Central America through the inclusion of pollen, macrofossil, and lake sediment records developed or compiled by Scheff and others (2017) and Shuman and Serravezza (2017).

Our proxy network includes records of soil, cave, and lake water chemistry, lake level fluctuations, and glacier mass-balance in addition to the vegetation-based records derived from lake and bog sediments and pack rat middens. For each record, we categorize the LGM (21 ± 2 ka) hydroclimatic response as "wetter," "drier," or "no change" relative to modern conditions. In categorizing proxy response, our designation is based on the original interpretation of the authors or the most recent compilations, as in the case of vegetation-based estimates (Scheff and others, 2017; Harbert and Nixon, 2018). Records for which no clear hydroclimatic designation can be made are coded as "unclear." Estimates of precipitation change from mountain glacier mass-balance modeling are only included in our compilation if they explicitly address uncertainties regarding the combined influence of temperature and precipitation change on glacier advance through independent estimates of temperature change (e.g., Laabs and others, 2006). Many glacier records are coded as unclear in our compilation due to uncertainties in the balance of temperature versus moisture variability.

We compare our network of precipitation-sensitive proxy records to the output of monthly climatologies for nine simulations of LGM (21 ka) climate conducted as part of phase 3 of the Paleoclimate Model Intercomparison Project (PMIP3) (Braconnot and others, 2012) accessed through the Earth System Grid Federation (ESGF) (Taylor and others, 2012). We use bilinear interpolation to calculate precipitation (P) and effective moisture (EM) values from annually summed precipitation and evapotranspiration of the 21-ka and Pre-Industrial (PI–0 ka) runs from the nine models in their native resolution using coordinates of the proxy record sites. For lakes we selected basin centers as representative coordinates. Additionally, we compare the proxy network to the ensemble average precipitation for the LGM and PI by averaging the P output of all models following interpolation to a 1° by 1° grid. We then calculate the annual P and EM anomalies for the LGM, expressed as percent, for each model and the ensemble using the equations:

$$P_{anom} = (P_{21ka}/P_{0ka}) \times 100 \quad (1)$$

$$EM_{anom} = (EM_{21ka}/EM_{0ka}) \times 100 \quad (2)$$

We compare the hydroclimatic changes simulated by each model and the ensemble with the change observed in each proxy record using a weighted Cohen's $\kappa_w$ statistic (e.g., DiNezio and Tierney, 2013; Oster and others, 2015; Hermann and others, 2018), which measures categorical data agreement between two raters who classify items (here proxy locations) into categories (wetter, drier, no change) relative to the probability of random agreement, and weights observations according to the degree of model-proxy disagreement (Cohen, 1968). This is accomplished by multiplying a matrix of model-proxy observations by a weight matrix in which strong agreement between observers (e.g., both model and proxy suggest wetter conditions at a site) is given a weight of 0, strong disagreement (e.g., the model suggests wetter, but the proxy drier) is given a weight of one, and weak disagreement (e.g., the model suggests wetter, but the proxy suggests no change) is given a weight of 0.5. $\kappa_w$ is then calculated as:

$$\kappa_w = 1 - \frac{\sum_{i=1}^{C}\sum_{j=1}^{C} w_{ij}x_{ij}}{\sum_{i=1}^{C}\sum_{j=1}^{C} w_{ij}m_{ij}} \qquad (3)$$

where:

$w_{ij}$ and $x_{ij}$ = elements in the weight and observed matrices, respectively
$m_{ij}$ = elements in the matrix of scores that would arise through random chance.

To identify the maximum possible agreement between models and proxies, we varied the threshold of change in P and EM required for the model responses to fall into the wetter or drier category from 5 to 35%. Computed $\kappa_w$ values can range from -1 to 1, where -1 is perfect disagreement, 0 is no agreement greater than random chance, and 1 is perfect agreement between the model and proxy records (Cohen 1968). For the EM $\kappa_w$ calculations, sites falling in grid cells that contain some proportion of ocean were excluded.

## RESULTS AND DISCUSSION

Our updated proxy network improves upon the spatial coverage of our previous compilation (Oster and others, 2015) by specifically increasing coverage in the Pacific Northwest and the Colorado Plateau, and also expanding the network to include records from the rest of the United States, Mexico, and northern Central America (figure 1). The updated network retains the clear wetter south–drier north dipole previously apparent in the western United States (Oster and others, 2015), but includes more records that variably suggest enhanced or reduced aridity at the LGM along the southern Colorado Plateau. Proxy records in the Midwest suggest wetter conditions, while those in the mid-south to the east coast of the United States as well as southern Mexico indicate no change in hydroclimatic conditions. Increased aridity during the LGM is suggested for Florida and parts of the deep South.

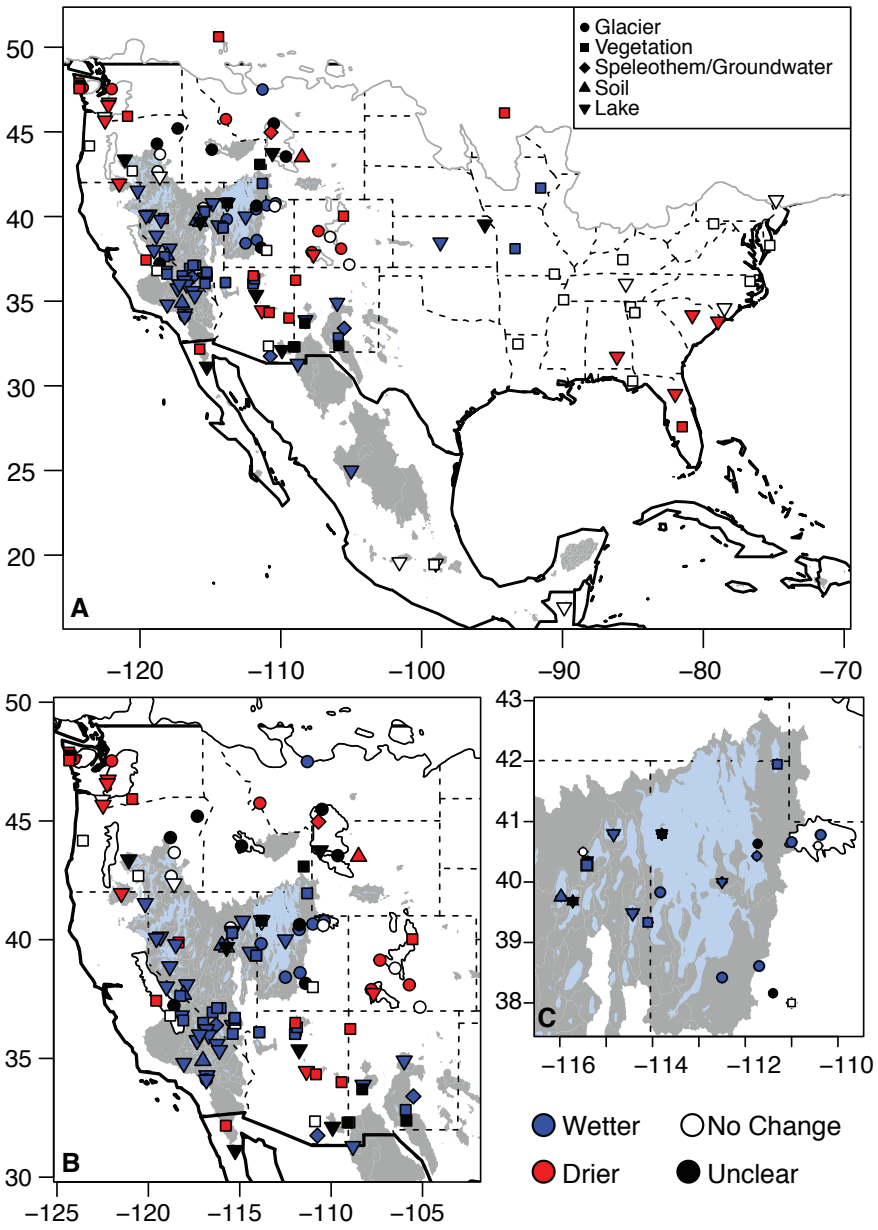


In our previous work, we identified a suite of five models that produced high $\kappa_w$ values when compared to our proxy network. These included IPSL-CM5A-LR, MPI-ESM-P, NCAR CCSM4, CNRM-CM5, and MIROC-ESM. The highest $\kappa_w$ for each of these models occurred at low thresholds for precipitation change (5–10%) (Oster and others, 2015). Many of the same models perform well in comparison with our updated proxy network, still at precipitation change thresholds of 5–10%. MPI-ESM-P has the highest $\kappa_w$ value, and NCAR CCSM4, IPSL-CM5A-LR, and MIROC-ESM have slightly lower $\kappa_w$ values (figure 2). The model COSMO-ASO, which was not among the models showing the best agreement previously, has the third highest $\kappa_w$ value in comparison with the expanded proxy network. The same five models have the highest $\kappa_w$ when considering a proxy network that is spatially limited to the western United States, providing a more direct comparison to the previous proxy network. In general, the models display

***Figure 1:*** *Proxy network for A) all of North and northern Central America, B) western United States, and C) area surrounding glacial Lake Bonneville. On all maps, proxies are denoted by type (shape) and LGM moisture conditions (color). The southern boundary of the LGM Laurentide and Cordilleran ice sheets are shown in white (Ehlers and others, 2011). Inward draining basins are shown in gray (Lehner and Grill, 2013; Ibarra and others, 2018), and the extent of pluvial lakes are shown in blue (http://www.naturalearthdata.com/downloads/10m; Soller and others, 2009).*

lower $\kappa_w$ values when anomalies in EM, rather than P, are considered. However, the models MRI-CGCM3 and CNRM-CM5, which are not among those with the highest precipitation $\kappa_w$ values, have the top values when considering EM anomalies (not shown). Interestingly, the ensemble average of P anomalies has a high $\kappa_w$ value (0.44) (figure 2). Only MPI-ESM-P has a higher precipitation $\kappa_w$ value (0.46) than the ensemble. The ensemble $\kappa_w$ , however, is highest for a much larger precipitation change threshold (20%) compared to the individual models. This means that a larger proportion of the study area falls into the "no change" category, reducing the number of sites where the model and proxies strongly disagree.

The majority of the high-scoring models and the ensemble simulate increased aridity across the eastern United States and in the Pacific Northwest and wetter conditions in the southwestern United States. As with our previous study, we find that differences in model agreement with the proxy network appear to be closely related to the location and geometry in the model simulations of the transition between wet anomalies in the southwestern United States and dry anomalies in the Pacific Northwest. This transition generally occurs near the California-Oregon border at 42 °N, stretching eastward across the northern Great Basin. In many of the models with higher $\kappa_w$ and in the ensemble, this transition from wet to dry precipitation anomalies trends from the northwest to the southeast across the western United States with varying degrees of undulation (figure 2). Areas of persistent disagreement between models and the proxy network may reflect a change in precipitation seasonality that is important for proxy response, but not apparent in the model annual averages used here. For instance, the aridity recorded by some proxies from the Colorado Plateau may reflect reduced monsoon rainfall during the LGM that is overshadowed in the annual model average by increased winter precipitation (e.g., Bhattacharya and others, 2018). Alternatively, apparent drying displayed by some vegetation-based proxies may primarily reflect reduced atmospheric $CO_2$ during the LGM rather than hydroclimatic change (Scheff and others, 2017).

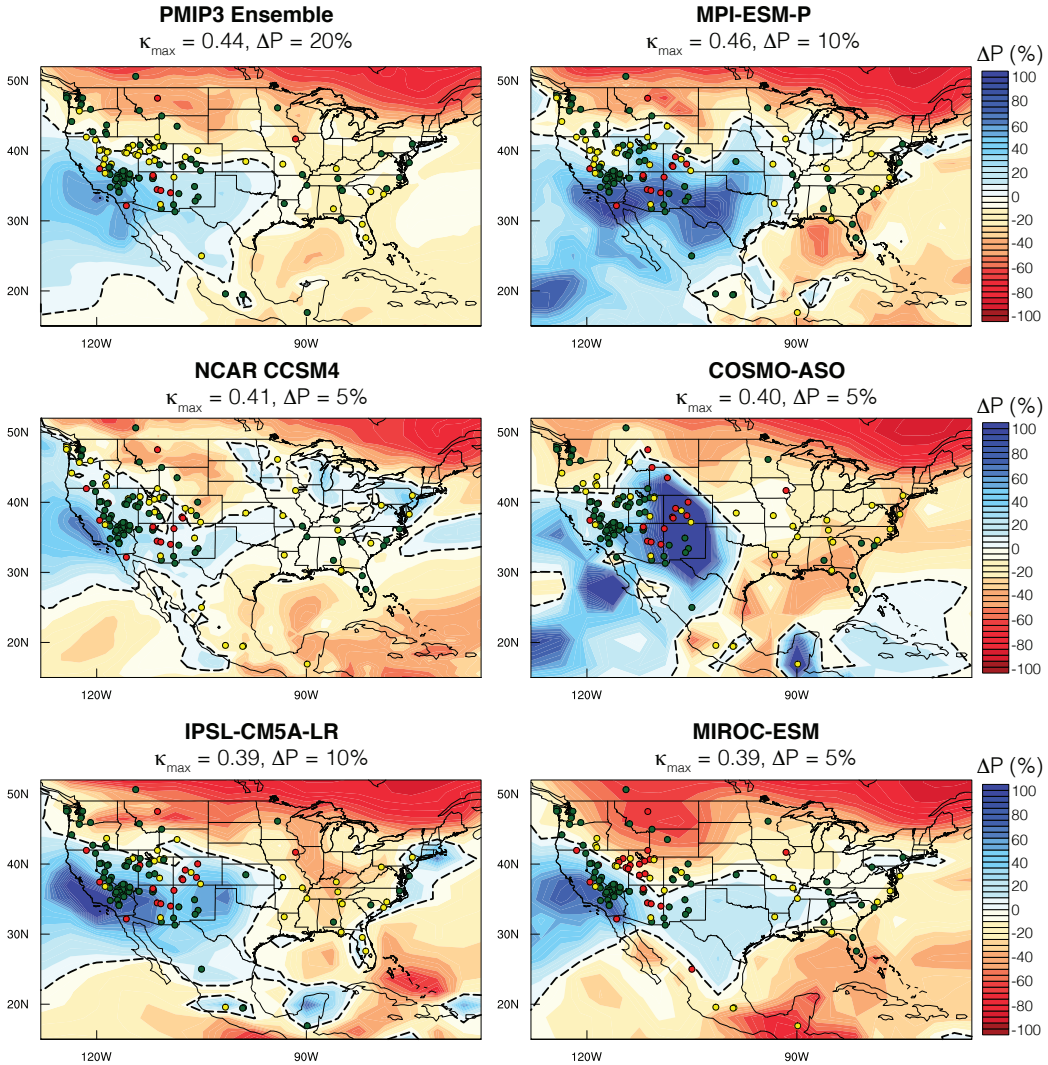


***Figure 2:*** *Contoured percentage change in annual precipitation (% ΔP, LGM-PI) with maximum $\kappa_w$ for the ensemble and the five models with the highest $\kappa_w$ values. Proxies shown as agreeing (green), weakly disagreeing (yellow), or strongly disagreeing (red) with each model at maximum $\kappa_w$. Contour line of zero ΔP is dashed for each model.*

Although we do not reanalyze atmospheric dynamics of these models here, this updated proxy-model comparison is consistent with our previous assertion that squeezing and deflection of zonal winds and steering of storms along a northwest to southeast trend due to the pressure gradient caused by the permanent high-pressure system over the Laurentide Ice Sheet was an important factor in determining the spatial pattern of hydroclimatic variation across the western United States at the LGM. We do not explicitly analyze the source of increased moisture to the western United States, though our results are not inconsistent with increased southwesterly moisture intruding into the continental interior as suggested by Lora and others (2017). Further analysis of atmospheric dynamics and moisture source changes across all of North and Central America will be conducted using this expanded proxy network and the LGM simulations associated with the updated PMIP4 modeling effort, scheduled to be released in 2019 (Kageyama and others, 2017).

Lake Bonneville occupies a critical position in the context of hydroclimatic change in western North America. Situated in the northeastern Great Basin between 37.5 and 43°N, Lake Bonneville is located within the transition zone between wetter and drier precipitation anomalies noted in both the proxy records and the models. Paleoclimate proxy records from the Bonneville basin, including records from pollen, tufa deposits, and ostracodes suggest conditions that were unchanged or slightly wetter during the LGM (Oviatt and others, 1992; Davis, 2002; Kaufman, 2003; Benson and others, 2011; McGee and others, 2012). Likewise, mass balance modeling of glaciers in the Wasatch Range and Uinta Mountains to the east of Lake Bonneville also point to an LGM that was either unchanged or slightly wetter (Munroe and Mickelson, 2002; Laabs and others, 2006; Refsnider and others, 2008; Quirk and others, 2018). The climate models with the highest $\kappa_w$ values place the transition from wet to dry LGM precipitation anomalies at or near the location of Lake Bonneville (figures 2 and 3), further suggesting that reduced evaporation in combination with small precipitation increases likely drove moderate to high lake levels in the northern Great Basin during the LGM (e.g., Reheis and others, 2014; Ibarra and others, 2014; 2018).

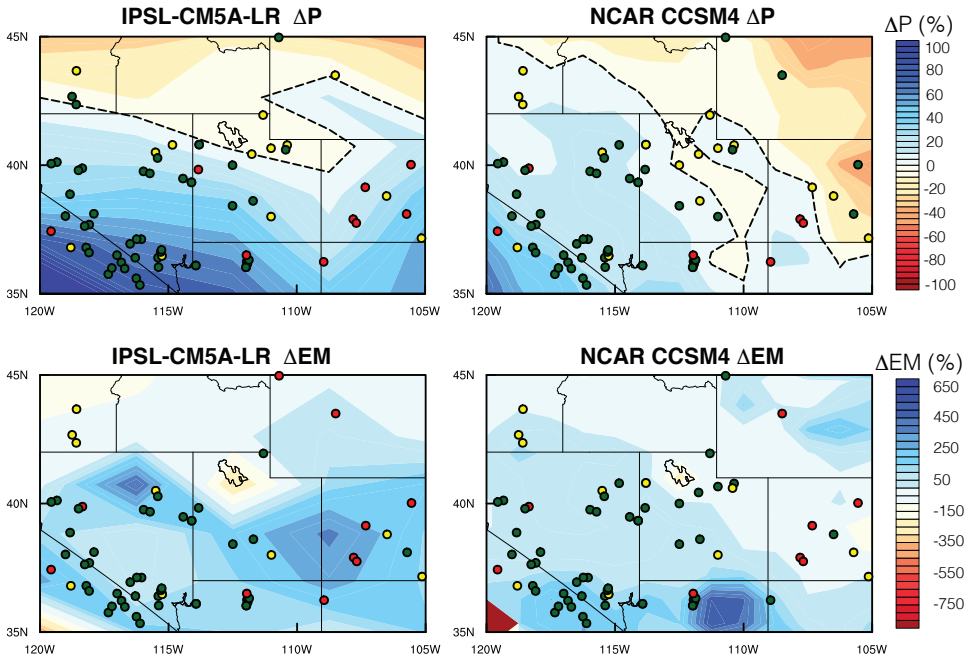


***Figure 3:*** *Contoured percentage change in annual precipitation (% ΔP, LGM-PI) (top panels), and EM (% ΔEM, LGM-PI) (bottom panels) for the models IPSL-CM5-LR and NCAR CCSM4 for the area surrounding Lake Bonneville. Proxy sites are colored as in figure 2. The negative anomaly polygons over the location of present-day Great Salt Lake for both models suggest that the lake is included in the land surface boundary conditions. Both models show positive precipitation anomalies downwind of the lake.*

Importantly, the PMIP models do not include Lake Bonneville or other pluvial lakes in their land surface boundary conditions, omitting potentially important moisture sources for regional mountain glacier growth. However, it is apparent from the computed EM anomalies, and indicated in the model set-up variables, that the present Great Salt Lake is included in the model boundary conditions for at least two of the models with higher $\kappa_w$ values, IPSL-CM5A and NCAR CCSM4 (figure 3). Interestingly, both of these models display a zone of higher LGM P anomalies just to the east of the Bonneville basin, downwind of Great Salt Lake, which is included in the model parameterization. These models display agreement to weak disagreement with the proxy records in the Bonneville basin, suggesting a narrow margin of small, positive P anomalies fueled by locally recycled vapor from Lake Bonneville is the most likely hydroclimate scenario for this region at the LGM. This observation underscores the influence that large pluvial lakes such as Bonneville and Lahontan must have had on their local hydroclimate (e.g., Hostetler and others, 1994; Galewsky, 2013), and the potential improvement to the simulation of vapor recycling effects and model-proxy agreement should these lakes be included in model boundary conditions (i.e., Pound and others, 2014) in the future.

## CONCLUSIONS

We have expanded the network of hydroclimatically sensitive paleoclimate proxy records from the LGM to include all of North America and northern Central America and to provide more detailed coverage of the western United States. We compare this updated proxy network to output of precipitation and effective moisture anomalies for the LGM (21 ka) simulations associated with PMIP3, as well as with an ensemble average. We find five models that have relatively high $\kappa_w$ for precipitation, all at low (5–10%) precipitation change thresholds. Only one model, MPI-ESM-P, has a higher $\kappa_w$ than the model ensemble. The ensemble $\kappa_w$ is highest at a larger (20%) change threshold, meaning it designates a larger part of the study area as experiencing no significant precipitation change relative to modern. Similar to our previous work, we find that proxy-model agreement is closely tied to the location and orientation of the boundary between wetter and drier conditions in the western United States. Lastly, although these models do not include pluvial lakes in their boundary conditions, EM anomalies indicate that at least two of the models that best agree with the proxy network likely do include Great Salt Lake. These two models show weak positive P anomalies downwind of the modern lake area, and are in general good agreement with Bonneville basin proxy records. This observation provides further evidence that modeling of vapor recycling and proxy-model agreement in the western United States could be improved with the inclusion of pluvial lakes in model boundary conditions for the LGM.

## ACKNOWLEDGMENTS

This work was funded by National Science Foundation grant AGS-1554998 to JLO. Data associated with the proxy network compilation are available from JLO by request. We gratefully acknowledge the international climate modeling groups participating in CMIP5/PMIP3 for making their model output available for analysis. We also acknowledge Neil Kelley and Cameron de Wet for discussion and suggestions.

## REFERENCES

Benson, L.V., Lund, S.P., Smoot, J.P., Rhode, D.E., Spencer, R.J., Verosub, K.L., Louderback, L.A., Johnson, C.A., Rye, R.O., and Negrini, R.M., 2011, The rise and fall of Lake Bonneville between 45 and 10.5 ka: Quaternary International, v. 235, p. 57–59.

Bhattacharya, T., Tierney, J.E., Addison, J.A., and Murray, J.W., 2018, Ice-sheet modulation of deglacial North American monsoon intensification: Nature Geoscience, v. 11, p. 848–852, doi:10.1038/s41561-018-0220-7.

Braconnot, P., Harrison, S.P., Kageyama, M., Bartlein, P.J., Masson-Delmotte, V., Abe-Ouchi, A., Otto-Bliesner, B., and Zhao, Y., 2012, Evaluation of climate models using palaeoclimatic data: Nature Climate Change, v. 2, p. 417–424, doi:10.1038/nclimate1456.

Cohen, J., 1968, Weighted kappa—nominal scale agreement with provision for scaled disagreement or partial credit: Psychological Bulletin, v. 70, p. 213–220.

COHMAP Members, 1988, Climatic changes of the last 18,000 years—observations and model simulations: Science, v. 241, p. 1043–1052.

Davis, O.K., 2002, Late Neogene environmental history of the northern Bonneville basin—a review of palynological studies, *in* Hershler, R., Curry, D., and Madsen, D., editors, Great Basin aquatic system history: Smithsonian Contributions to the Earth Sciences, v. 33, p. 295–307.

DiNezio, P.N., and Tierney, J.E., 2013, The effect of sea level on glacial Indo-Pacific climate: Nature Geoscience, v. 6, p. 485–491.

Ehlers, J., Gibbard, P.L., and Hughes, P.D., 2011, Quaternary glaciations—Extent and chronology, A Closer Look: Amsterdam, Elsevier, 1108 p.

Galewsky, J., 2013, High-resolution paleoclimate simulations of Lake Bonneville and its influence on geomorphic processes in the Uinta Mountains during the Last Glacial Maximum [abs.]: American Geophysical Union Fall Meeting, San Francisco December 9-13, abstract EP51C-04, http://abstractsearch.agu.org/meetings/2013/FM/EP51C-04.html.

Harbert, R.S., and Nixon, K.C., 2018, Quantitative late Quaternary climate reconstruction from plant macrofossil communities in Western North America: Open Quaternary, v. 4, p. 8, doi:10.5334/oq.46.

Hermann, N.W., Oster, J.L., and Ibarra, D.E., 2018, Spatial patterns and driving mechanisms of mid-Holocene hydroclimate in western North America: Journal of Quaternary Science, v. 33, p. 421–434, doi:10.1002/jqs.3023.

Hostetler, S.W., Giorgi, F., Bates, G.T., and Bartlein, P.J., 1994, Lake-atmosphere feedbacks associated with paleolakes Bonneville and Lahontan: Science, v. 263, p. 665–668.

Ibarra, D.E., Egger, A.E., Weaver, K.L., Harris, C.R., and Maher, K., 2014, Rise and fall of late Pleistocene pluvial lakes in response to reduced evaporation and precipitation—Evidence from Lake Surprise, California: Geological Society of America Bulletin, v. 126, p. 1387–1415, doi:10.1130/B31014.1.

Ibarra, D.E., Oster, J.L., Winnick, M.J., Caves Rugenstein, J.K., Byrne, M.P., and Chamberlain, C.P., 2019, Lake area constraints on past hydroclimate in the western United States—Application to Pleistocene Lake Bonneville, *in* Lund, W.R., McKean, A.P., and Bowman, S.D., editors, Proceedings volume 2018 Lake Bonneville geologic conference and short course: Utah Geological Survey Miscellaneous Publication 170.

Kageyama, M., Albani, S., Braconnot, P., Harrison, S.P., Hopcroft, P.O., Ivanovic, R.F., Lambert, F., Marti, O., Peltier, W.R., Peterschmitt, J.-Y., Roche, D.M., Tarasov, L., Zhang, X., Brady, E.C., Haywood, A.M., LeGrande, A.N., Lunt, D.J., Mahowald, N.M., Mikolajewicz, U., Nisancioglu, K.H., Otto-Bliesner, B.L., Renssen, H., Tomas, R.A., Zhang, Q., Abe-Ouchi, A., Bartlein, P.J., Cao, J., L., Q., Lohmann, G., Ohgaito, R., Shi, X., Volodin, E., Yoshida, K., Zhang, X., Zheng, W., 2017, The PMIP4 contribution to CMIP6, Part 4—Scientific objectives and experimental design of the PMIP4-CMIP6 Last Glacial Maximum experiments and PMIP4 sensitivity experiments: Geoscientific Model Development, v. 10, p. 4035–4055, doi:10.5194/gmd-10-4035-2017.

Kaufman, D.S., 2003, Amino acid paleothermometry of Quaternary ostracodes form the Bonneville basin, Utah: Quaternary Science Reviews, v. 22, p. 899–914.

Laabs, B.J.C., Plummer, M.A., and Mickelson, D.M., 2006, Climate during the last glacial maximum in the Wasatch and southern Uinta Mountains inferred from glacier modeling: Geomorphology, v. 75, p. 300–317.

Lehner, B., and Grill, G., 2013, Global river hydrography and network routing: baseline data and new approaches to study the world's largest river systems: Hydrological Processes, v. 27, p. 2171–2186.

Lora, J.M., Mitchell, J.L., Risi, C., and Tripati, A.E., 2017, North Pacific atmospheric rivers and their influence on western North America at the Last Glacial Maximum: Geophysical Research Letters, v. 44, p. 1051–1059, doi: 10.1002/2016GL071541.

Lyle, M., Heusser, L., Ravelo, C., Yamamoto, M., Barron, J., Diffenbaugh, N.S., Herbert, T., and Andreasen, D., 2012, Out of the tropics—The Pacific, Great Basin lakes, and late Pleistocene water cycle in the western United States: Science, v. 337, p. 1629–1633.

Maher, K., Ibarra, D.E., Oster, J.L., Miller, D.M., Redwine, J.L., Reheis, M.C., and Harden, J.W., 2014, Uranium isotopes in soils as a proxy for past infiltration and precipitation across the western United States: American Journal of Science, v. 314, p. 821–857.

McGee, D., Quade, J., Edwards, R.L., Broecker, W.S., Cheng, H., Reiners, P.W., and Evenson, N., 2012, Lacustrine cave carbonates—Novel archives of paleo-hydrologic change in the Bonneville basin (Utah, USA): Earth and Planetary Science Letters, v. 351, p. 182–194, doi: 10.1016/j.epsl.2012.07.019.

Morrill, C., Lowry, D.P., and Hoell, A., 2018, Thermodynamic and dynamic causes of pluvial conditions during the Last Glacial Maximum in western North America: Geophysical Research Letters, v. 45, p. 335–345.

Munroe, J.S., and Laabs, B.J.C., 2013, Temporal correspondence between pluvial lake highstands in the southwestern US and Heinrich Event 1: Journal of Quaternary Science, v.28, p. 49–58, doi:10.1002/jqs2586.

Munroe, J.S., and Mickelson, D.M., 2002, Last Glacial Maximum equilibrium-line altitudes and paleoclimate, northern Uinta Mountains, Utah, U.S.A: Journal of Glaciology, v. 48, p. 257–266.

Natural Earth pluvial lakes database: http://www.naturalearthdata.com/downloads/10m-physical-vectors/10m-lakes/.

Nowak, C.L., Nowak, R.S., Tausch, R.J., and Wigand, P.E., 1994, Tree and shrub dynamics in northwestern Great Basin woodland and shrub steppe during the late Pleistocene and Holocene: American Journal of Botany, v. 81, p. 265–277, doi:10.1002/j.1537-2197.1994.tb15443.x.

Oster, J.L., Ibarra, D.E., Winnick, M.J., and Maher, K., 2015, Steering of westerly storms over western North America at the Last Glacial Maximum: Nature Geoscience, v. 8, p. 201–205, doi: 10.1038/ngeo2365.

Oviatt, C.G., Currey, D.R., and Sack, D., 1992, Radiocarbon chronology of Lake Bonneville, eastern Great Basin, USA: Palaeogeography, Palaeoclimatology, Palaeoecology, v. 99, p. 225–241.

Pound, M.J., Tindall, J., Pickering, S.J., Haywood, A.M., Dowsett, H.J., and Salzmann, U., 2014, Late Pliocene lakes and soils–A global dataset for the analysis of climate feedbacks in a warmer world: Climate of the Past, v. 10, p. 167–180, doi:10.5194/cp-10-167-2014.

Quirk, B.J., Moore, J.R., Laabs, B.J.C., Caffee, M.W., and Plummer, M.A., 2018, Termination II, Last Glacial Maximum, and late glacial chronologies and paleoclimate from Big Cottonwood Canyon, Wasatch Mountains, Utah: Geological Society of America Bulletin, v. 130, p. 1889–1902, doi: 10.1130/B31967.1.

Refsnider, K.A., Laabs, B.J.C., Plummer, M.A., Mickelson, D.M., Singer, B.S., and Caffee, M.W., 2008, Last glacial maximum climate inferences from cosmogenic dating and glacier modeling of the western Uinta ice field, Uinta Mountains, Utah: Quaternary Research, v. 69, p. 130–144.

Reheis, M.C., Adams, K.D., Oviatt, C.G., and Bacon, S.N., 2014, Pluvial lakes of the western United States—a view from the outcrop: Quaternary Science Reviews, v. 97, p. 33–37.

Scheff, J., Seager, R., Liu, H., and Coats, S., 2017, Are glacials dry? Consequences for paleoclimatology and for greenhouse warming: Journal of Climate, v. 30, p. 6593–6609.

Shuman, B.N., and Serravezza, M., 2017, Patterns of hydroclimatic change in the Rocky Mountains and surrounding regions since the last glacial maximum: Quaternary Science Reviews, v. 173, p. 58–77.

Soller, D.R., Reheis, M.C., Garrity, C.P., and Van Sistine, D.R., 2009, Map database for surficial materials in the conterminous United States: U.S. Geological Survey Data Series 425, scale 1: 5,000,000.

Taylor, K.E., Stouffer, R.J., and Meehl, G.A., 2012, An overview of CMIP5 and the experiment design: Bulletin of the American Meteorological Society, v. 93, p. 485–498.

**This content is a PDF version of the author's PowerPoint presentation.**